

Comparative N₂ Fixation Performance of Diverse Micro- and Nanosized 2D Materials Measured by Gas Chromatography

Jijoe Samuel Prabagar¹, Joonwoo Seo¹ and Dong-Kwon Lim^{1,2,3,*}

¹ KU-KIST Graduate School of Converging Science and Technology, Korea University, 145 Anam-ro, Seongbuk-gu, Seoul 02841, Republic of Korea

² Department of Integrative Energy Engineering, Korea University, 145 Anam-ro, Seongbuk-gu, Seoul 02841, Republic of Korea

³ Brain Science Institute, Korea Institute of Science and Technology (KIST), 5, Hwarang-ro 14-gil, Seongbuk-gu, Seoul 02792, Republic of Korea

* Corresponding author. E-mail: dklim@korea.ac.kr

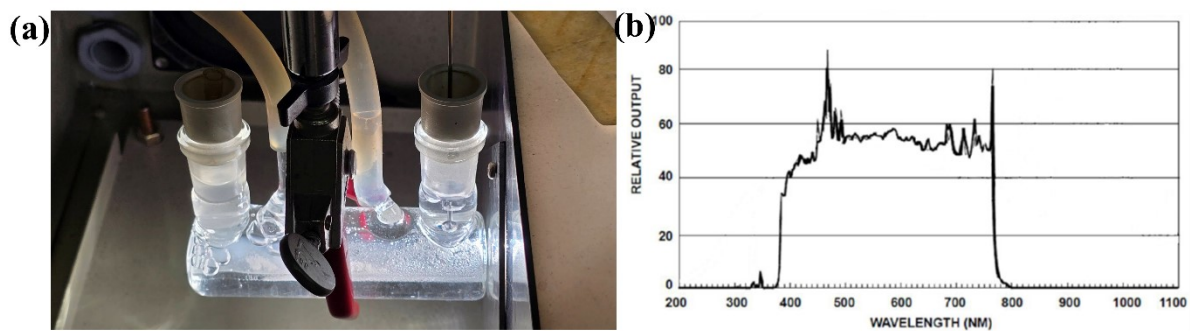


Fig. S1 (a) Experimental set-up for photocatalytic generation of ammonia employing Xe lamp with a water circulation jacket and (b) Spectrum of light from the Xe lamp (400–780 nm).

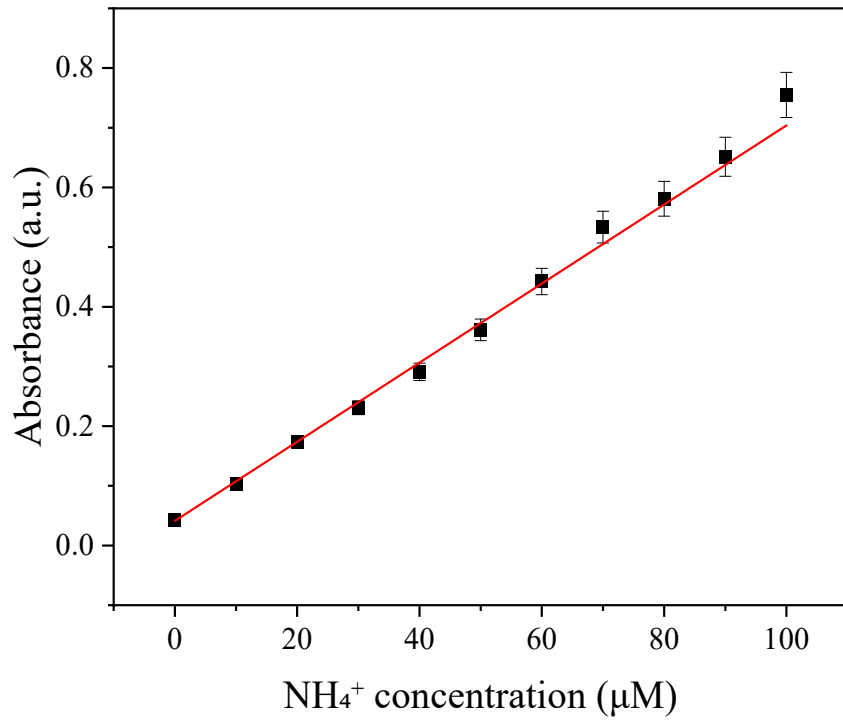


Fig. S2 Linear relationship between the absorbance at 650 nm and the NH₄⁺ concentration.

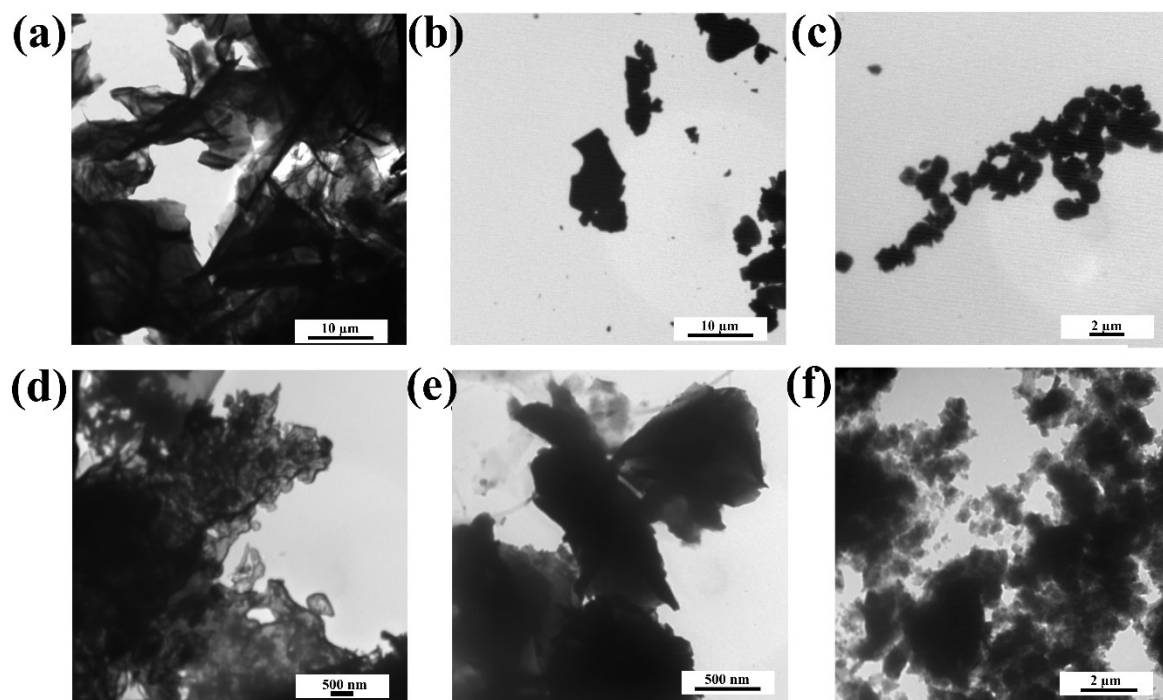


Fig. S3 TEM image of micro-sized 2D synthesized (a) rGO, (b) MXene, (c) Bi₂O₃, (d) gC₃N₄, (e) In₂S₃ and (f) Ni-MOF.

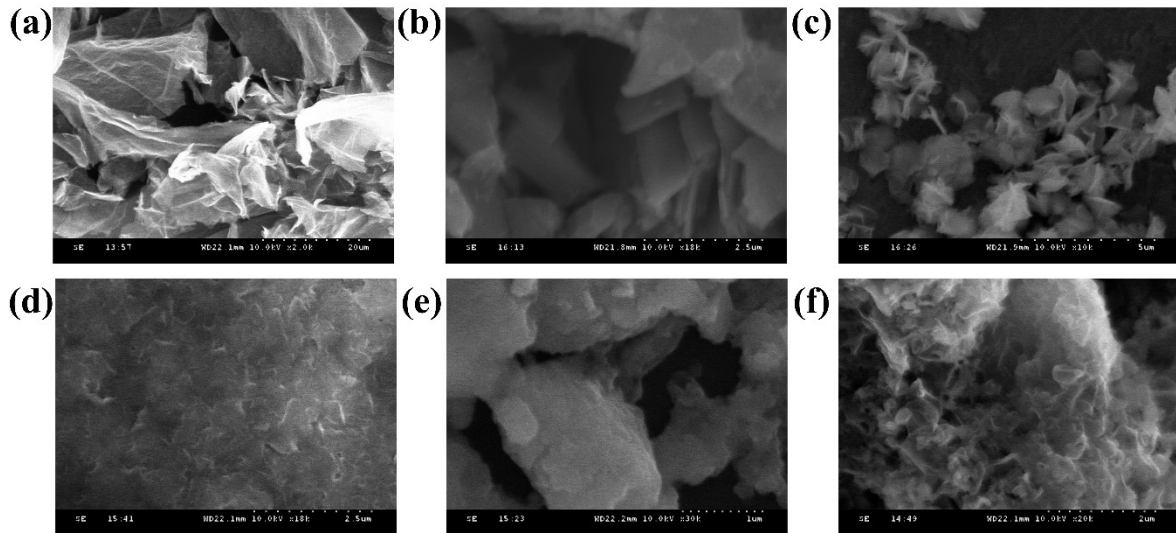


Fig. S4 SEM image of micro-sized 2D synthesized (a) rGO, (b) MXene, (c) Bi₂O₃, (d) gC₃N₄, (e) In₂S₃ and (f) Ni-MOF.

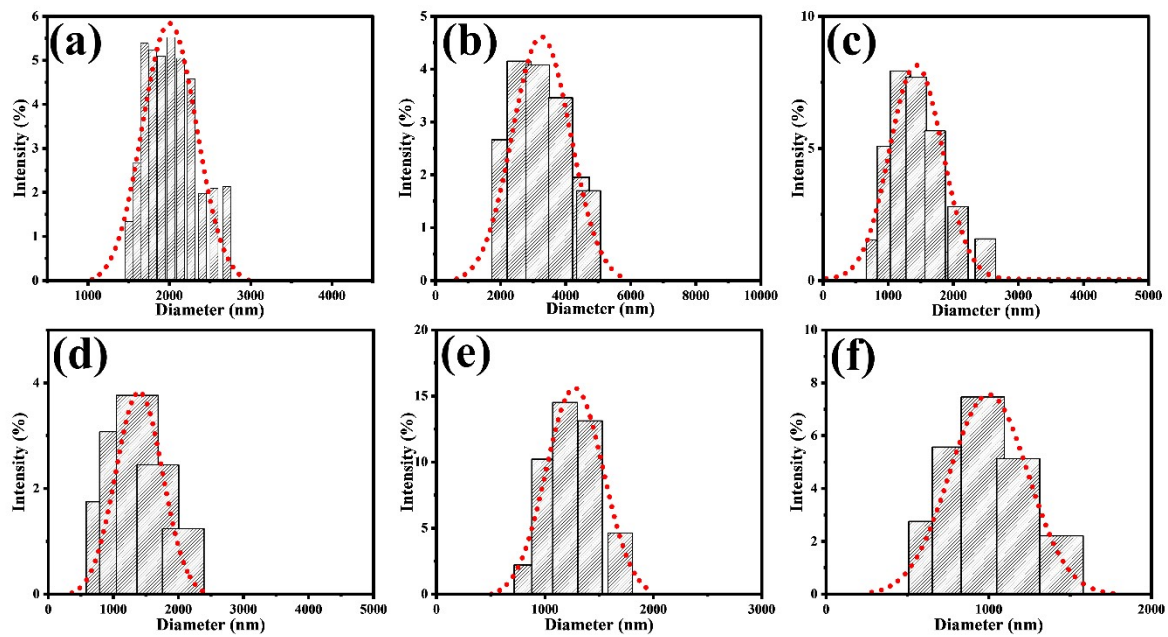


Fig. S5 Particle size analysis of micro-sized (a) rGO, (b) MXene, (c) Bi₂O₃, (d) gC₃N₄, (e) In₂S₃ and (f) Ni-MOF.

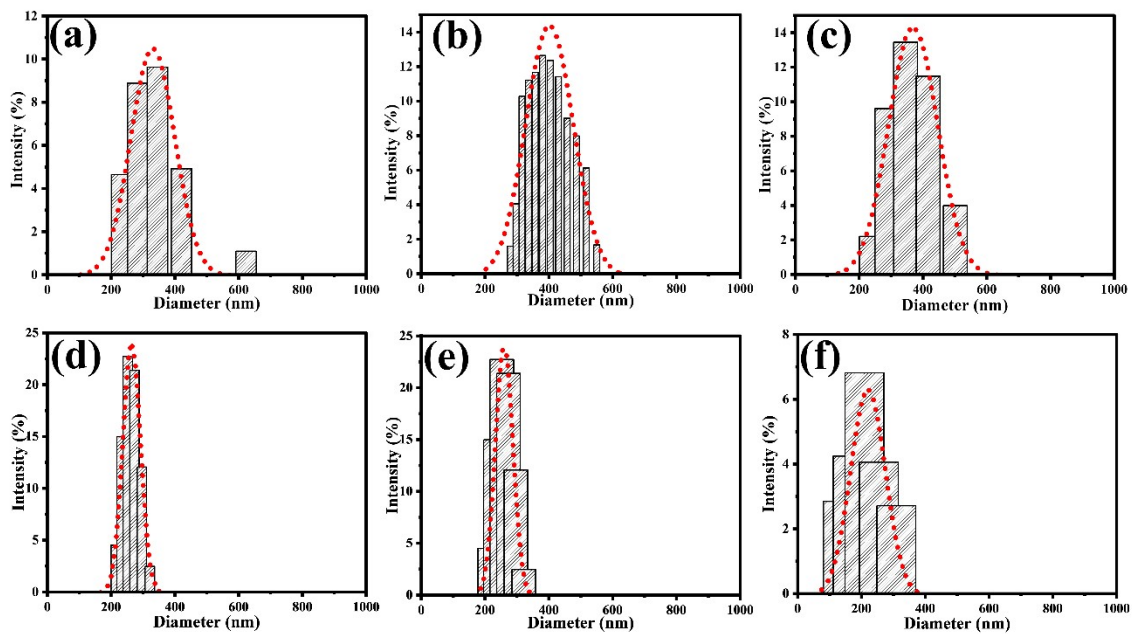


Fig. S6 Particle size analysis of nano-sized (a) rGO, (b) MXene, (c) Bi₂O₃, (d) gC₃N₄, (e) In₂S₃ and (f) Ni-MOF. The data confirms the successful fabrication of nano-sized materials achieved through the sonication technique.

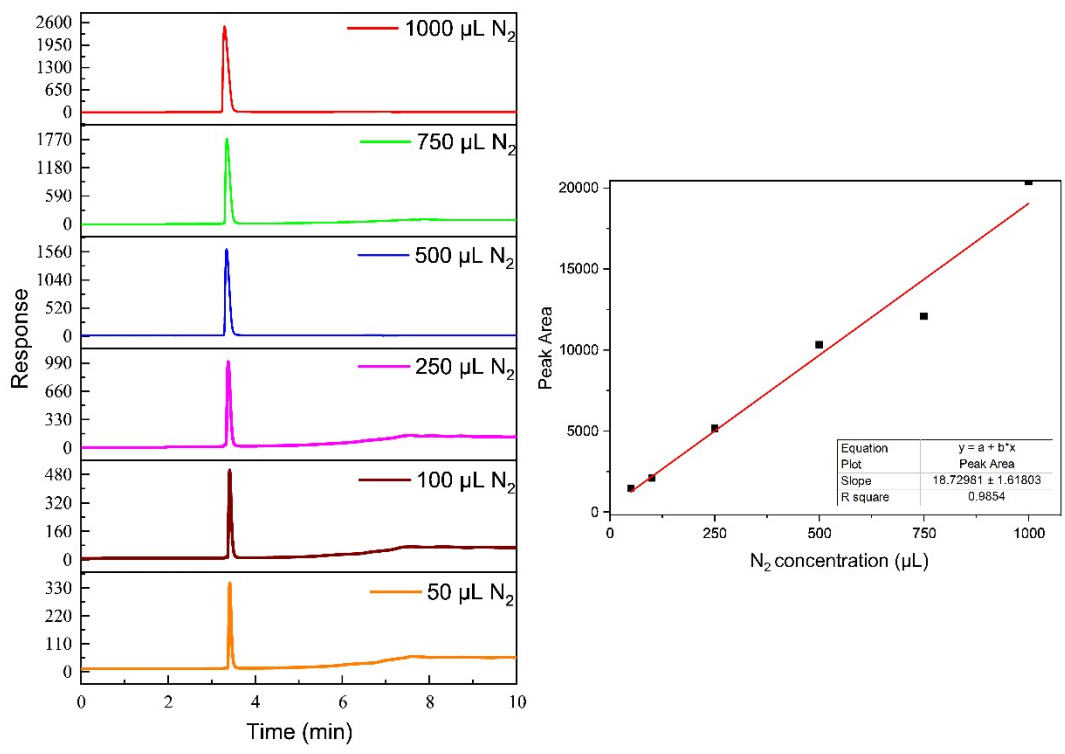


Fig. S7 Varying N₂ concentration peaks with the corresponding linear calibration curve (right), used to determine the unknown N₂ concentration.

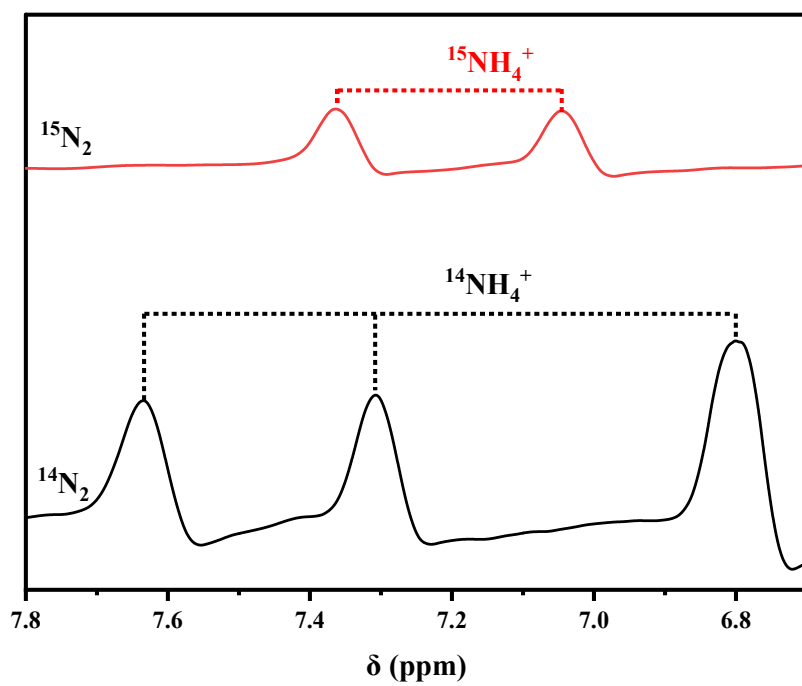


Fig. S8 ^1H NMR spectra of $^{14}\text{NH}_4^+$ and $^{15}\text{NH}_4^+$ produced from using $^{14}\text{N}_2$, $^{15}\text{N}_2$.

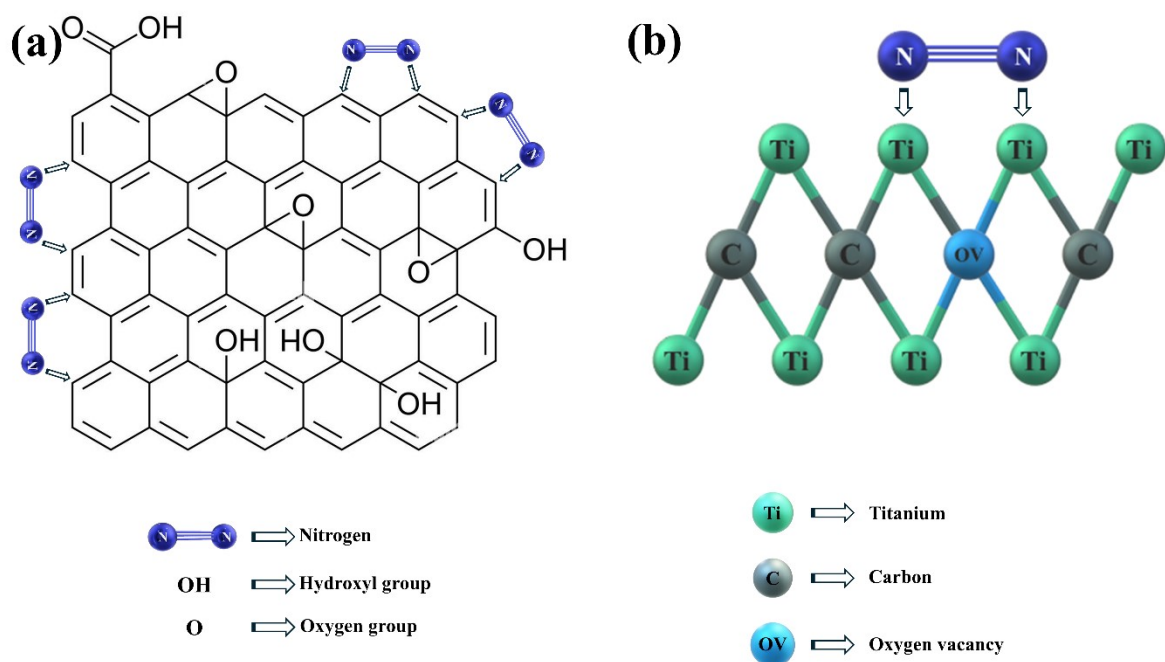


Fig. S9 Probable N_2 fixation mechanism on broken carbon edges of (a) rGO forming both 5-membered pyrazole and 6-membered pyridazine and (b) MXene via end-on mode (Ti) along with side-on mode on OV.

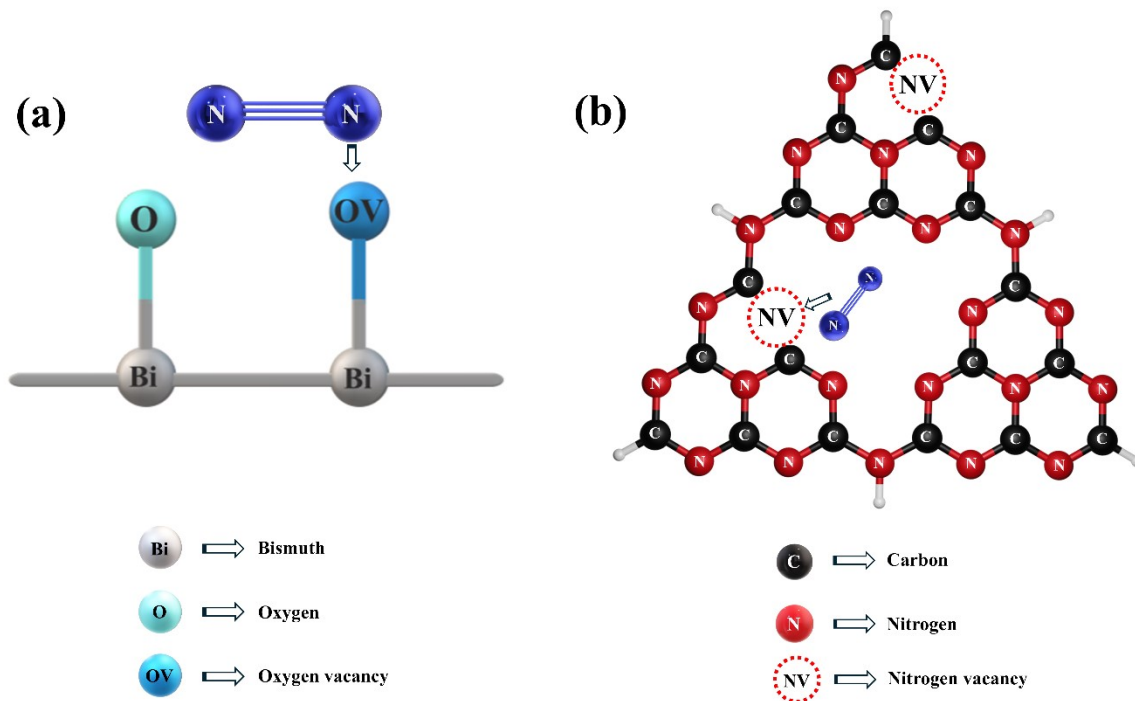


Fig. S10 Probable N_2 fixation mechanism on (a) Bi_2O_3 through available OVs and (b) gC_3N_4 through NVs.

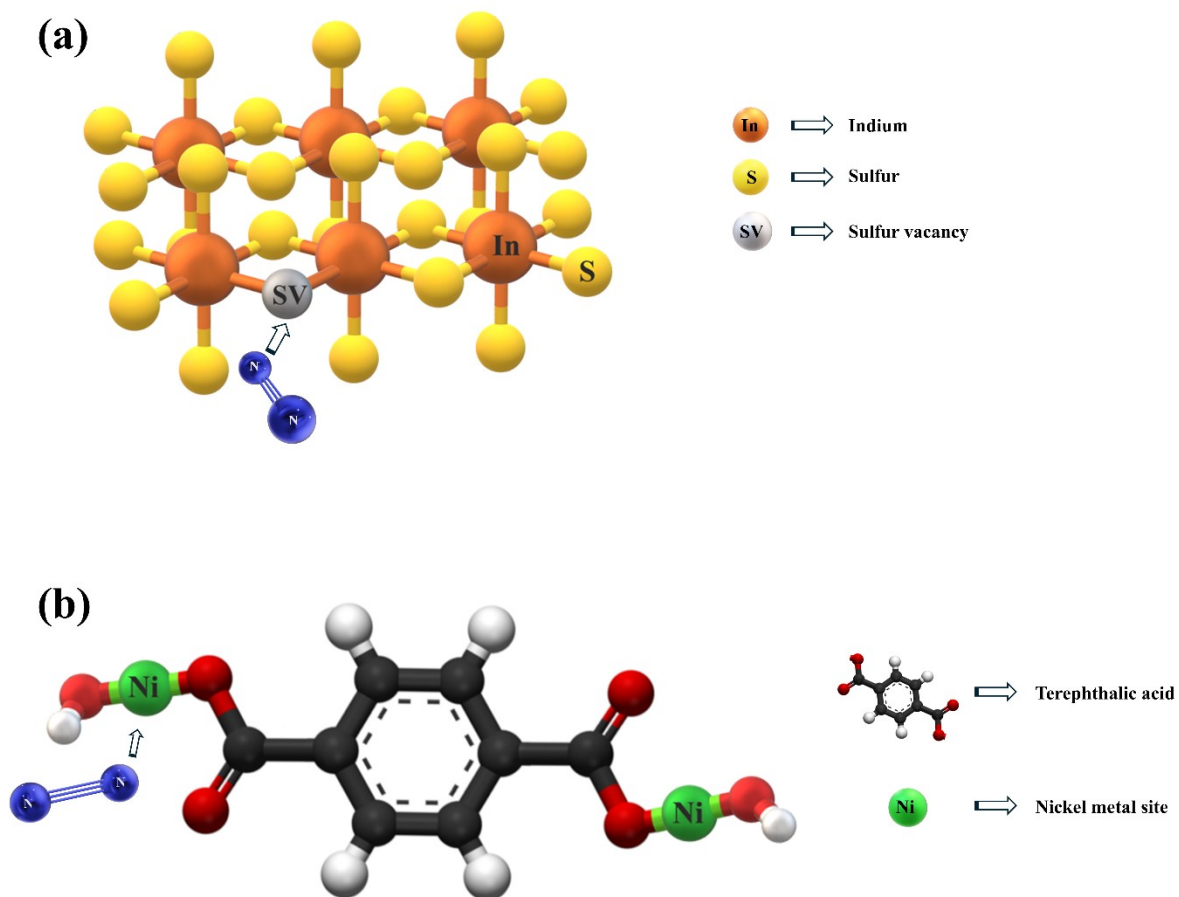


Fig. S11 Probable N_2 fixation mechanism on (a) In_2S_3 via SVs, and (b) Ni-MOF utilizing active metal sites.

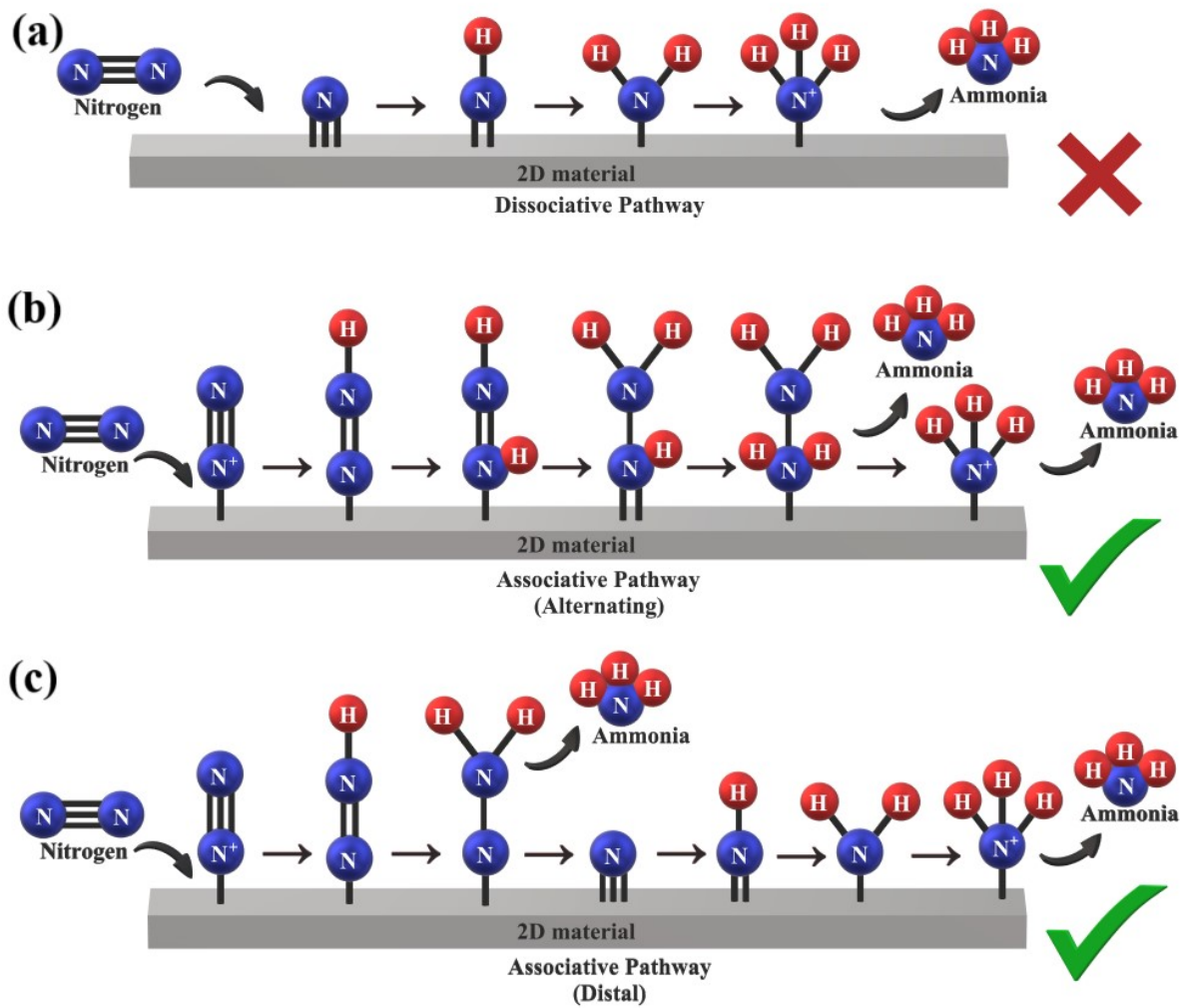


Fig. S12 The three pathways for ammonia generation: (a) dissociative pathway, (b) alternating associative pathway, and (c) distal associative pathway, where the photocatalytic reaction follows either the alternating or distal associative pathway.

Table S1 Gibbs free energy (ΔG) for the highest efficient gC_3N_4 with NVs and the lowest efficient Ni-MOF with metal active sites

Intermediate steps in N_2 conversion	$\Delta G_{gC_3N_4}$ (eV)	ΔG_{Ni-MOF} (eV)
$* + N_2 \rightarrow *N_2$	-0.73	0.3
$*N-N + e^- + H^+ \rightarrow *N-NH$	-1.74	1.74
$*N-NH + e^- + H^+ \rightarrow *N-NH_2$	-2.46	1.66
$*N-NH_2 + e^- + H^+ \rightarrow *N + NH_3$	-3.9	1.53
$*N + e^- + H^+ \rightarrow *NH$	-4.06	2.41
$*NH + e^- + H^+ \rightarrow *NH_2$	-3.19	0.37
$*NH_2 + e^- + H^+ \rightarrow NH_3$	-2.11	-1.22